World Journal of Gastroenterology

Online Submissions: http://www.wjgnet.com/esps/
wjg@wjgnet.com
doi:10.3748/wjg.v19.i5.692

World J Gastroenterol 2013 February 7; 19(5): 692-705
ISSN 1007-9327 (print) ISSN 2219-2840 (online)

ORIGINAL ARTICLE

Comparison of different methods of intestinal obstruction in a rat model

Meng-Lang Yuan, Zheng Yang, Yu-Cheng Li, Lan-Lan Shi, Jia-Ling Guo, Yu-Qin Huang, Xia Kang, Jing-Jing Cheng, Yang Chen, Ting Yu, De-Qi Cao, Huan Pang, Xiao Zhang

Meng-Lang Yuan, Yu-Cheng Li, Jia-Ling Guo, Yu-Qin Huang, Xia Kang, Jing-Jing Cheng, Huan Pang, Department of Clinical Medicine, Chengdu Medical College, Chengdu 610081, Sichuan Province, China
Zheng Yang, Xiao Zhang, Lan-Lan Shi, Department of Experimental Technology, Chengdu Medical College, Chengdu 610081, Sichuan Province, China
Yang Chen, Ting Yu, Department of Pharmaceutics, Chengdu Medical College, Chengdu 610081, Sichuan Province, China
De-Qi Cao, Department of Laboratory Medicine, Chengdu Medical College, Chengdu 610081, Sichuan Province, China
Author contributions: Yuan ML and Yang Z contributed equally to this work; Yang Z designed the study; Yuan ML, Guo JL, Huang YQ, Kang X and Cheng JJ performed the majority of experiments; Chen Y, Yu T, Li YC and Cao DQ collected and analyzed the data; Yuan ML and Yang Z wrote the manuscript; Yang Z, Shi LL, Pang H and Zhang X reviewed the paper.
Supported by Higher Education Quality Project of Sichuan Province: Innovative Scientific Experiment Project of Sichuan Province, Grant No. SJCX201110; Chengdu Medical College Innovative Scientific Experiment Project, Grant No. CX201220 and CX201115
Correspondence to: Zheng Yang, Experimentalist, Department of Experimental Technology, Chengdu Medical College, Chengdu 610081, Sichuan Province, China. yz3191021@yahoo.com.cn
Telephone: +86-28-68289174 Fax: +86-28-68289152
Received: September 25, 2012 Revised: December 24, 2012
Accepted: January 5, 2013
Published online: February 7, 2013

Abstract

AIM: To investigate different methods of creating incomplete intestinal obstruction in a rat model and to compare their electrophysiologic, morphologic and histologic characteristics.

METHODS: Rat ileum was partially obstructed by the respective application of: braided silk (penetrated the mesentery and surrounded intestine); half ligation (penetrated directly and ligated 1/2 cross-section of the intestine); wide pipe (6 mm in width, surrounded the intestine); narrow pipe (2 mm in width, surrounded the intestine). A control was also included (no obstruction). Various behavioral and electrophysiologic variables, as well as morphologic and immunohistochemical observations were recorded by blinded investigators at different time points (12, 24, 48, 72 h), including daily general condition, ileal wet weight and circumference, macromorphous and micromorphous intestine, bowel movement capability *in vivo* and *in vitro*, slow wave and neural electrical activity, and the number of c-Kit positive interstitial cells of Cajal (ICC).

RESULTS: Despite being of a similar general condition, these methods resulted in different levels of obstruction in each group compared with the control at different time points (12, 24, 48, 72 h). However, these fields of the wide pipe rat showed significantly differences when compared with the other three obstructed groups at 12 to 72 h, including macroscopic and histological presentation, intestinal transit ratio and contractility, circumference and wet weight, amplitude and frequency of nerve electrical discharge and slow wave, and ICC numbers (all $P < 0.01$).

CONCLUSION: The wide pipe rat method is significantly more reliable and stable than the other methods of obstruction, demonstrating that use of the wide pipe method can be a useful model of incomplete intestinal obstruction.

Key words: Intestinal obstruction; Model; Comparative study; Electrophysiology; Morphology; Interstitial cells of Cajal

Yuan ML, Yang Z, Li YC, Shi LL, Guo JL, Huang YQ, Kang X, Cheng JJ, Chen Y, Yu T, Cao DQ, Pang H, Zhang X. Comparison of different methods of intestinal obstruction in a rat model. *World J Gastroenterol* 2013; 19(5): 692-705 Available from: URL: http://www.wjgnet.com/1007-9327/full/v19/i5/692.htm DOI: http://dx.doi.org/10.3748/wjg.v19.i5.692

INTRODUCTION

Intestinal obstruction (IO) is one of the most common diseases in abdominal surgery. It can slowly lead to changes in intestinal structure and function, and in extreme cases it can be life-threatening[1,2]. Incomplete intestinal obstruction is the initial phase of intestinal obstruction and is the clinical pathological basis for other types of intestinal obstruction. In addition, when considering the impairment associated with incomplete intestinal obstruction, exploring its diagnosis and treatment has important clinical significance.

Animal models of incomplete intestinal obstruction are important in the investigation of the pathogenic mechanisms involved in human intestinal obstruction, and play an important role in identifying and testing novel interventions. To date, animal models of incomplete intestinal obstruction have included mice, rats, rabbits, pigs and approximately six other types of animals[3-5]. No particular model parallels the complex nature of human intestinal obstruction. The drawback of using animal models is that the basis for the high rate of incomplete intestinal obstruction is not known.

Therefore, it is necessary to establish a reliable animal model to study the pathogenesis of intestinal obstruction, and to have a good experimental model to allow the exploration, research and ultimate treatment of intestinal obstruction. Different types of materials to induce obstruction are currently available. The prosthetic valve has been used since 1996[5]. This was followed by half ligation using braided silk, which was developed in 2004 and has been available since 2008. One report describes the changes elicited by ligating the intestines outside the body[4]. A 24-Fr latex T-tube, cut to form a pipe, was used in China to establish a model of intestinal obstruction[6].

With regard to species selection, the anatomy and physiology of primates are similar to humans, but due to ethical and economic limitations this model is not widely used. Whichever method or species is selected, the ideal animal model should be similar and comparable to the human disease, demonstrate repeatability, be economic and easy to use[7]. In this study, rats were selected and three different materials were used to establish intestinal obstruction.

Based on the above factors, the purpose of the present experimental study was to compare the characteristics of four methods of incomplete intestinal obstruction in the rat model. In addition, we also obtained electrophysiologic, morphologic and histologic information on each method which may have clinical relevance.

MATERIALS AND METHODS

Animals

Healthy adult female and male Sprague-Dawley rats, weighing between 180 and 280 g, were provided by the Laboratory Animal Center [Licence No. SCXK (CHUAN) 2006-10; Sichuan University, Chengdu, China], and were individually housed at 22 ℃ in a 12-h light/dark cycle, with free access to tap water and a standard pellet diet (Laboratory Animal Center, Sichuan University, Chengdu, China) for at least 1 wk before the start of the experiments.

Surgical procedure

One hundred and fifty rats were randomly divided into five groups of thirty in each group. 12 h prior to each study, the animals were fasted but had free access to water, and were anesthetized with 1.5% pentobarbital sodium (30 mg/kg body weight, intraperitoneal; Beijing Chemical Reagent, batch number, 090205; Beijing, China). In this study, a loop of intestine was exposed, and partially obstructed using the respective material. Three different materials were used to obstruct the intestine. A round needle with braided silk No. 0 (Pudong Jinhuan Medical Products, batch number, 11L02028; Shanghai, China) penetrated the mesentery, a polyethylene pipe (2 mm exterior diameter) was placed at the side of the intestine and a ligature was formed with the braided silk, the pipe was then pulled out smoothly from the ligation. This group was known as the braided silk group. Braided silk No. 3-0 (Pudong Jinhuan Medical Products, batch number, 11L02028; Shanghai, China) was used to directly penetrated the intestine and ligate 1/2 cross-section of the intestine. This group was known as the half ligation group. A 24-Fr latex T-tube (Nantong Angel Medical Instruments, batch number, 20110304; Jiangsu, China) was cut to form a pipe 10 mm in length and 6 mm in width which surrounded the intestine. This group was known as the wide pipe group. In another group of rats, a narrow pipe 10 mm in length and 2 mm in width was used to obstruct the intestine. This group was known as the narrow pipe group. The rings were located in the ileum 20 mm oral to the ileocecal sphincter, and this was followed by closure of the abdomen. All materials were placed with the cut side between the lateral extensions of the mesenteric vascular bed to avoid vascular injury[3]. The control group underwent a similar procedure, but the rings used in these animals were 10 mm in length and did not result in occlusion of the ileum.

Postoperative care

After surgery, the animals were treated with an intraperitoneal injection of a 2 mL mixture of glucose (9 mg/mL; Shuanghe Pharmaceutical Industry, batch number,

Table 1 Criteria for scoring macromorphous intestinal damage

Feature	Description	Score
Adhesions	None	0
	Slight, ileum can be separated from other tissues with little effort	1
	Involved in a number of intestinal loops	2
Stenosis	None	0
	Slight	2
	Severe, proximal intestinal distention	3
Ulceration	None	0
	Damage extended to < 1 cm along the length at one site	1
	Damage extended to < 1 cm along the length at two sites	2
	Damage extended to > 1 cm along the length at one siteor multiple lesions	3
Bowel wall thickness	< 1 mm	0
	1-3 mm	1
	> 3 mm	2
Total score		10

Table 2 Criteria for scoring micromorphous intestinal damage

Feature	Description	Score
Ulceration	None	0
	Ulceration < 3 mm, no hyperemia or focal hyperemia, no ulceration	1
	Ulceration < 3 mm, with focal hyperemia or ulceration > 3 mm, without hyperemia	2
	Ulceration > 3 mm or hyperemia	3
Inflammation	None	0
	Slight	1
	Moderate	2
	Severe	3
Fibrogenesis	None	0
	Slight	1
	Severe	2
Extent of involved bowel wall	None	0
	Submucosa	1
	Muscular layer and even serosa	2
Total score		10

100829 6K; Anhui, China) and sodium chloride (50 mg/mL; Shuanghe Pharmaceutical Industry, batch number, 100825 1E; Anhui, China) in a ratio of 1:1 (vol/vol), and 0.1 mL potassium chloride (100 mg/mL; Jiaozuo Pharmaceutical Industry, batch number, 11031641; Tianjin, China). The animals were then allowed to recover on a heated blanket. The rats were allowed to fast 2 h before the last administration, and were rapidly euthanized with pentobarbital sodium at 12, 24, 48, and 72 h, respectively. The abdomen was then cut open and the test was started.

Daily general condition

After surgery, the rats were housed in individual cages. Each day at approximately 9 AM, body weight and food intake were recorded, and feces were collected from each cage. The number of feces pellets was counted and color was observed. Feces from each rat were then lyophilized and weighed to determine fecal dry weight. The total number and dry weight of the fecal pellets were calculated. The mental status and death of rats were recorded.

Measurement of ileum circumference and wet weight

Following sacrifice of the rats, a 3 cm fresh intestinal segment was obtained, the intestinal contents were removed using Tyrode's solution, the segment was then dried with filter paper, and ileal weight was recorded. The ileal wet weight index was calculated using the fasting body weight (kg) divided by the weight (g) of the 3 cm intestinal segment. A bowel segment (10 cm) cut longitudinally along the opposite side of the mesenteric edge was obtained, and its circumference was measured at three sites, and the average was recorded.

Morphological studies

The ileum was opened by an incision along the mesenteric border and laid flat. Tissue damage was assessed and was scored on the 3 cm intestinal segment which was taken 5 cm oral to the ileus, using the criteria outlined in Tables 1 and 2 adapted from Butzner *et al*[8]. Each section was then graded by two blinded observers. Scoring was based on a number of features which were scored from 0 to 10 depending on the presence and severity of visible ileal damage, which consisted of the extent and severity of adhesions, stenosis, ulceration, and bowel wall thickness. A score of 0 to 10 was used to describe the total scores of ulceration, inflammation, fibrogenesis and extent of bowel wall involved. Finally, the extent of histological intestinal mucosal damage was evaluated according to the grading system of Chiu *et al*[9].

Hematoxylin and eosin staining

Histological analysis of intestinal damage was carried out on pieces of muscle taken the same distance from the site of occlusion adjacent to the tissue regions used for electrophysiology. The intestinal tissues in Tyrode's solution were pinned. Connective tissues were removed, cut and pinned into a rectangular shape (1 cm × 2 cm, width and length). The ileal tissues were then fixed in 4% paraformaldehyde for 6 h at room temperature (RT). Two longitudinal sections, 1 cm in length and 2 mm thick, were taken from each fixed tissue segment. These sections were rinsed for 2 h in running water, dehydrated through a graded series of alcohols and embedded in paraffin using the Intelligent Program-controlled Automatic Hydroextractor of Biological Organization (Xiaogan Taiwei Science and Technology Industry, Hubei, China) and a tissue embedding console system (Jinhua Kedi Instrumental Equipment, Zhejiang, China). All paraffin-embedded tissue blocks were sectioned at 5 μm thickness using a microtome (Microsystems Nussloch; Leica Instruments, Shanghai, China), and slides were then prepared. The paraffin was removed from the slides by treatment with xylene. Sections were rehydrated with an ethanol series and stained with hematoxylin and eosin

and examined by light microscopy.

Bowel movement capability analysis

After the rats had fasted for 4 h, all groups received 3% activated charcoal suspension (Sigma, Aldrich, United States) in saline (1.5 mL/rat, *po*) as a charcoal meal. One hour after administration of the marker, the animals were anesthetized with an intraperitoneal injection (2 mL/kg) of pentobarbital sodium, and the small intestine from the pylorus sphincter to the ileocecal sphincter was removed. The intestinal transit ratio was calculated using the percentage of the small intestine length divided by the length the charcoal had travelled.

After the animals had been killed, the small intestine was exposed by a mid-line abdominal incision, and a 3 cm tubular segment of intestine was obtained 1 cm oral to the ileus. The bowel was opened along the mesenteric border and the intestinal contents were rinsed with Tyrode's solution. Segments from a 2 cm piece of bowel were cut and the mucosa was removed by sharp dissection. Strips of muscle (20 mm × 5 mm) were pinned to the hook and contractions were measured isometrically under a resting tension of 0.5-1 g in a 20 mL tissue chamber (Chengdu Technology and Market, Sichuan, China) containing Tyrode's solution for at least 30 min. A force transducer coupled to the BL-420F Biological Function Experimental System (Chengdu Technology and Market, Sichuan, China) was used to record the contractility of the ileum. The settings for the tension pattern was: scanning speed, 2.56 s/div, power gain, 2000, time constant, 5 s, and high-frequency filtering, 3 Hz. The sustained record time was up to 30 min, followed by 30 s of recorded data. Frequency and amplitude were recorded and calculated.

Measurement of neural electrical activity

Along the central line of the neck, a longitudinal cut open to the skin, layer by layer separating the muscles, fascia, and exposing the carotid sheath was made. After separating the vagus nerve, the nerve was immersed in 37 ℃ warm paraffin (Jiangcheng Lipid Chemical Industry, batch number, 100101; Jilin, China) and insulated with the surrounding tissue to prevent the nerve drying during recording. The recording electrodes were hooked to the vagus nerve, the reference electrode was placed on the skin fold, and the electrode input was connected to the BL-420F Biological Function Experimental System. The settings for the neural discharge pattern were: scanning speed, 80 ms/div, power gain, 10 000, time constant, 0.1 s, and high-frequency filtering, 1 KHz. As mentioned above, both frequency and amplitude were recorded.

Determination of slow wave

Ileal slow waves were measured using electrophysiology. A pair of self-made silver electrodes (5 mm in length, 0.1 mm in diameter) was implanted into the seromuscular layer of the intestine. The distance between the electrodes was about 5 mm and they were 10-20 mm away from the ring. The reference electrode was placed on the skin fold, the terminal was wired and connected to the BL-420F Biological Function Experimental System. A layer of paraffin gauze was used to cover the exposed ileum. The settings for the slow electrical signals pattern were: scanning speed, 1.28 s/div, power gain, 2000, time constant, 5 s, and high frequency filtering, 30 Hz. The sustained record time was up to 30 min, followed by 30 s of recorded data. Ten periods were then randomly intercepted using the modified Tomita method[10], and both frequency and amplitude were recorded, calculated and compared (as described earlier).

Immunohistochemistry

The expression of c-Kit in ileal tissue was assessed by immunohistochemistry. Specimens were fixed in 4% paraformaldehyde, dehydrated, and embedded in paraffin, as described previously. A mixed liquid suspension containing 5 mL garlic juice and fresh egg white was added to 100 mL glycerol, which was then used to coat a glass slide. The tissues were then deparaffinized in xylene and rehydrated in a descending ethanol series. After dewaxing and rehydration, antigen retrieval was performed using high pressure for 2 min, and then blocked by incubation in 3% H_2O_2 for 15 min at 37 ℃ to ablate endogenous peroxidase. The sections were washed in phosphate-buffered saline (PBS; 0.01 mol/L, pH 7.4), and then incubated with goat anti-c-Kit specific polyclonal antibody (sc-1494, 1:100, Santa Cruz, Biotechnology, United States) for 1 h at 37 ℃ in a wormwall incubator (Huyueming Instrument, Guangzhou, China). The slides were washed in PBS (5 × 3 min), and then incubated with a horseradish-peroxidase-conjugated rabbit anti-goat IgG(H+L) (Zhongshan Golden Bridge Biotechnology, Beijing, China) for 40 min at 37 ℃, rinsed (5 × 3 min) in PBS, and the sections were colored with 3,3-diaminobenzidine, kept at RT in the dark for 30 s. Following that, the slides were counterstained with hematoxylin, differentiated with 5 g/L hydrochloric ethanol, 1:400 ammonia recurrented blue, sequential ethanol dehydration, and then clearing and mounting with neutral resin. In the negative control the same steps as previously described were carried out, but the primary antibody was replaced by PBS. The positive expression of c-Kit in interstitial cells of Cajal (ICC) was shown by dotted dark brown cells with a nucleus or individual processes of dark brown rods.

Statistical analysis

All data were presented as means ± SE. P values < 0.01 were considered statistically significant. Each intestinal segment was taken from individual animals. The electrical parameters of each segment were analyzed: (1) frequency; (2) amplitude; and (3) contraction capability (contraction frequency multiplied by amplitude). A one-way ANOVA

test was used to compare parameters and the Kruskal Wallis test was used to compare parameters displaying abnormal distribution among the groups. Tukey's Honestly Significant Difference (HSD) test was used to detect the group causing variation when comparing qualitative data, and the Mann Whitney *U* test was used to detect the group causing variation. χ^2 or Fisher's exact test was used to compare qualitative data. All analyses were performed using SPSS 13.0 for Windows (SPSS Inc, United States). Adobe Photoshop 8.0 (Adobe, Mountain View, CA, United States) was used to construct and display the figures made from digital photos.

RESULTS

Clinical

Body weight, food intake, feces, mental status as well as mortality were recorded every 12 h. Of the average values in the control group, body weight, food intake, feces, mental status and death showed a wider band change from 12 to 24 h, this index showed a narrower band change from 24 to 72 h. Mean body weight, food intake, feces, mental status and death in the four different obstructed groups showed significant changes with persistent loss or gain ($P < 0.01$). The general condition of the rats is shown in Table 3.

Macroscopic and histological evaluation

The rings were placed on the ileum 20 mm oral to the ileocecal sphincter, which resulted in visible intestinal damage 12 to 72 h after surgery. In the control rats, no marked gross morphological changes in the intestine were observed (Figure 1A). However, morphological observation of the intestines revealed adhesions, stenosis, ulceration and bowel wall thickness of the rings to varying degrees in the rats with obstruction. In addition, flushing, tumefaction of intestinal mucosa, hyperemia and hemorrhage of bowel wall and stasis of bowel contents from the proximal region to the site of the ring were noted (Figure 1B-E). Figure 1F shows analytical data of the total scores of intestinal damage following macroscopic evaluation in obstructed and control rats.

The histological findings in ileal tissues are presented in Figure 2. No marked changes were observed in the control rats (Figure 2A). Histological observation of the intestines showed some features (including ulceration, inflammation, fibrogenesis and extent of involved bowel wall) of obstruction to varying degrees. As shown in Figure 2B-E, ulceration in the mucosa and submucosa, mucosal edema and inflammation, vascular congestion with focal hemorrhage from the mucosa to the muscular layer and even the serosa, occasional fibrogenesis, and infiltration of polymorphonuclear cells, plasma cells and neutrophils were observed. Figure 2F shows analytical data of the total scores of intestinal damage following histological evaluation and the scores of histological mucosal damage in obstructed and control rats. In the obstructed intestine, there was a marked increase in the thickness of the muscle layers. However, no apparent inflammatory changes, such as marked leucocyte infiltration of the tunica muscularis, were observed.

Circumference and wet weight of the intestine

After removing the intestine, 3 cm dilated intestinal segments were blotted with filter paper and weighed on an analytical balance. The sections were cut longitudinally and the circumference was measured at three sites. The average values for the ileal wet weight (Figure 3A) and ileal circumference (Figure 3B) in the dilated portion of the obstruction rat tissue were significantly larger ($P < 0.01$) than those in the corresponding portion of the controls.

Ileal contractility

We examined the contractile response of the obstructed and control rats, and the study was evaluated in terms of absolute force (mN per mg tissue wet weight). We also examined spontaneous contractile activity of the intestinal segments using isometric force measurements. Figure 4A-B shows the typical spontaneous contractile activity of the dilated intestine isolated from obstructed and control rats, which demonstrated that the slow form of the intestinal segments from control rats was regular; in contrast, the slow form of the intestinal segments from the obstructed rats at 12 to 72 h was attenuated and irregular to varying degrees. Analytical data of the intestinal transit ratio were obtained at four different time points and are shown in Figure 4C.

Autonomic nerve electrical discharge

Typical autonomic electrical activity of the vagus nerve was determined in obstructed and control rats *in vivo*, which indicated that the slow form of the vagus nerve autonomic electrical discharge in control rats was normal (Figure 5A); however, the slow form in obstructed rats at 12 to 72 h was attenuated and irregular to varying degrees (Figure 5B-C). At various time points, the obstructed group showed significant differences in nerve electrical discharge frequency and amplitude compared with the control group ($P < 0.01$). When the four groups were compared, the differences in the wide pipe group appeared to be most obvious, followed by the braided silk group, the half ligation and the narrow pipe group.

Ileum myoelectricity

The myoelectric changes in the ileum of each rat were determined (Figure 6A). The intestinal segments from the control rats did not show significant differences at the various time points, and the slow form was regular. In contrast, the obstructed rats showed significant reductions in vagus nerve electrical discharge frequency and amplitude ($P < 0.01$), the reduction in the wide pipe group was most obvious, followed by the braided silk group, the half ligation and the narrow pipe group. The

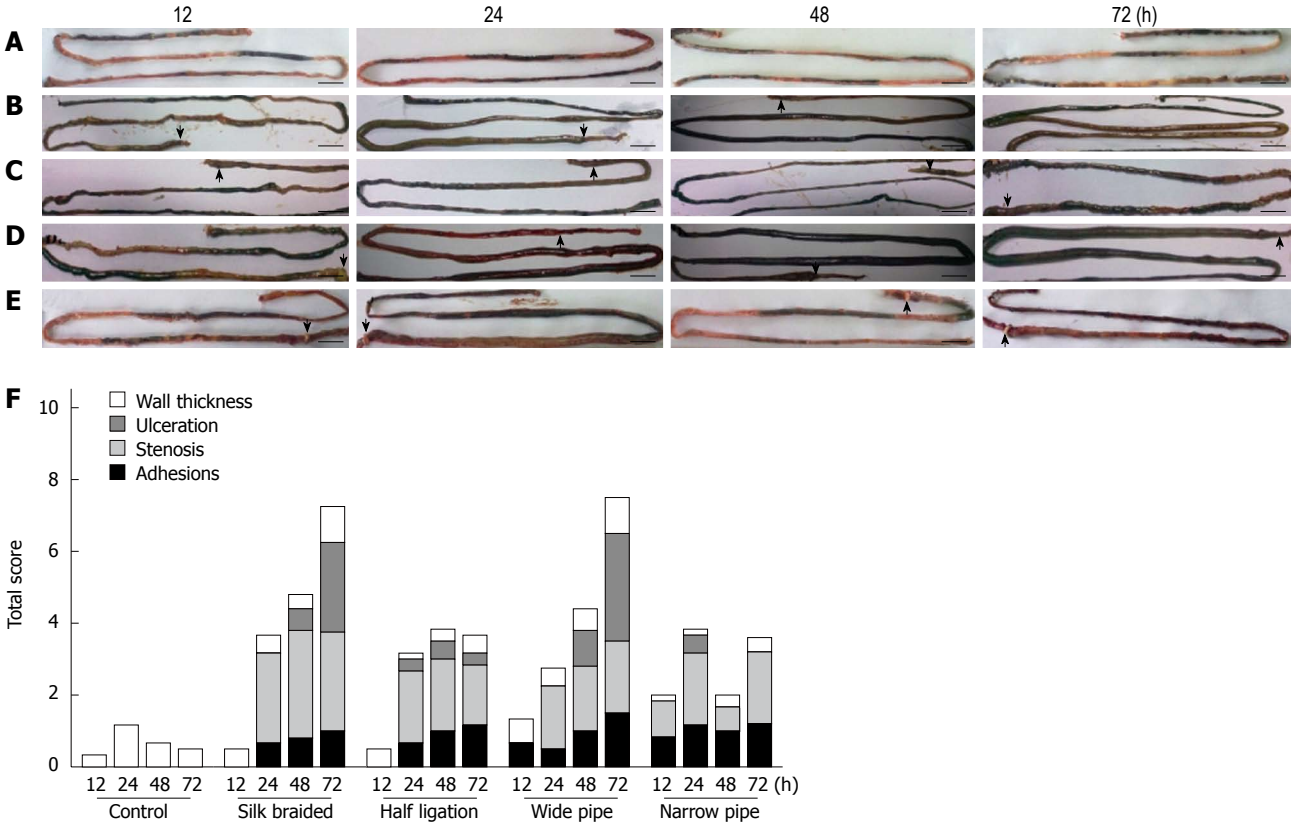

Figure 1 Dissection of the entire intestine from the pyloric antrum to the ileocecal valve in the obstructed and control rats. A: Control; B: Braided silk; C: Half ligation; D: Wide pipe; E: Narrow pipe. Rats were killed at different time points after surgery; F: The morphological score of changes in the extent and severity of adhesions, stenosis, ulceration and bowel wall thickness. The arrow indicates the portion of obstructed intestine bearing a ring (scale bar: 1 cm).

waveform of the dilated intestinal segment at 12 to 72 h was irregular to varying degrees and the appearance of a notching wave resembled a sine curve. The amplitude of the slow waves in the different groups was compared and is shown in Figure 6C. Amplitude and frequency values of the slow waves were significantly different in the obstructed group compared with the control group (both $P < 0.01$). Slow-wave amplitude was significantly reduced ($P < 0.01$) at all sites tested after surgery compared with the control rats. Frequency was reduced only at 72 h at the obstructed sites (Figure 6B).

ICC networks in the intestine

ICC networks are widely distributed within the submucosal (ICC-SM), intramuscular (ICC-IM, ICC-DMP) and inter-muscular layers (ICC-MY)[11,12]. Interestingly, the ICC-MY play an important role in the myenteric plexus and are characteristic of intestinal ICC. The control rats exhibited a dense network in the ICC-MY region of intestinal tissue from 12 to 72 h (Figure 7A), whereas the ICC-MY appeared to be greatly disrupted or absent in the obstructed rat tissue (Figure 7B-E). Analysis of c-Kit-like immunopositive cells in the obstructed rats showed that the immunopositive cells were significantly decreased compared with control animals.

DISCUSSION

An animal model is a reliable method of studying disease mechanisms and to test the effectiveness of a variety of therapeutic measures. Although the pathogenesis of intestinal obstruction is known, complete simulation of the pathology to establish an animal model of incomplete intestinal obstruction is difficult. In recent years, a number of studies have been published, such as that conducted by Chang *et al*[3], where the authors established incomplete intestinal obstruction in a mouse model by placing a polyethylene clip onto the intestine. The morphological and electrophysiological changes which occurred proximal to the site of the clip were investigated. Won *et al*[13] used a silicon tube to partially obstruct the ileum, and observed changes in intestinal contractility associated with the immunologically activated components.

In the present study, all rings were successfully placed to produce incomplete obstruction of the ileum. 12 to 72 h after obstruction, daily behavior did not significantly change in the control group, however, different daily behaviors were seen in the rats with intestinal obstruction (Table 3). In the obstructed rats, a significant reduction in body weight was observed ($P < 0.01$), which was most obvious in the narrow pipe group followed by the

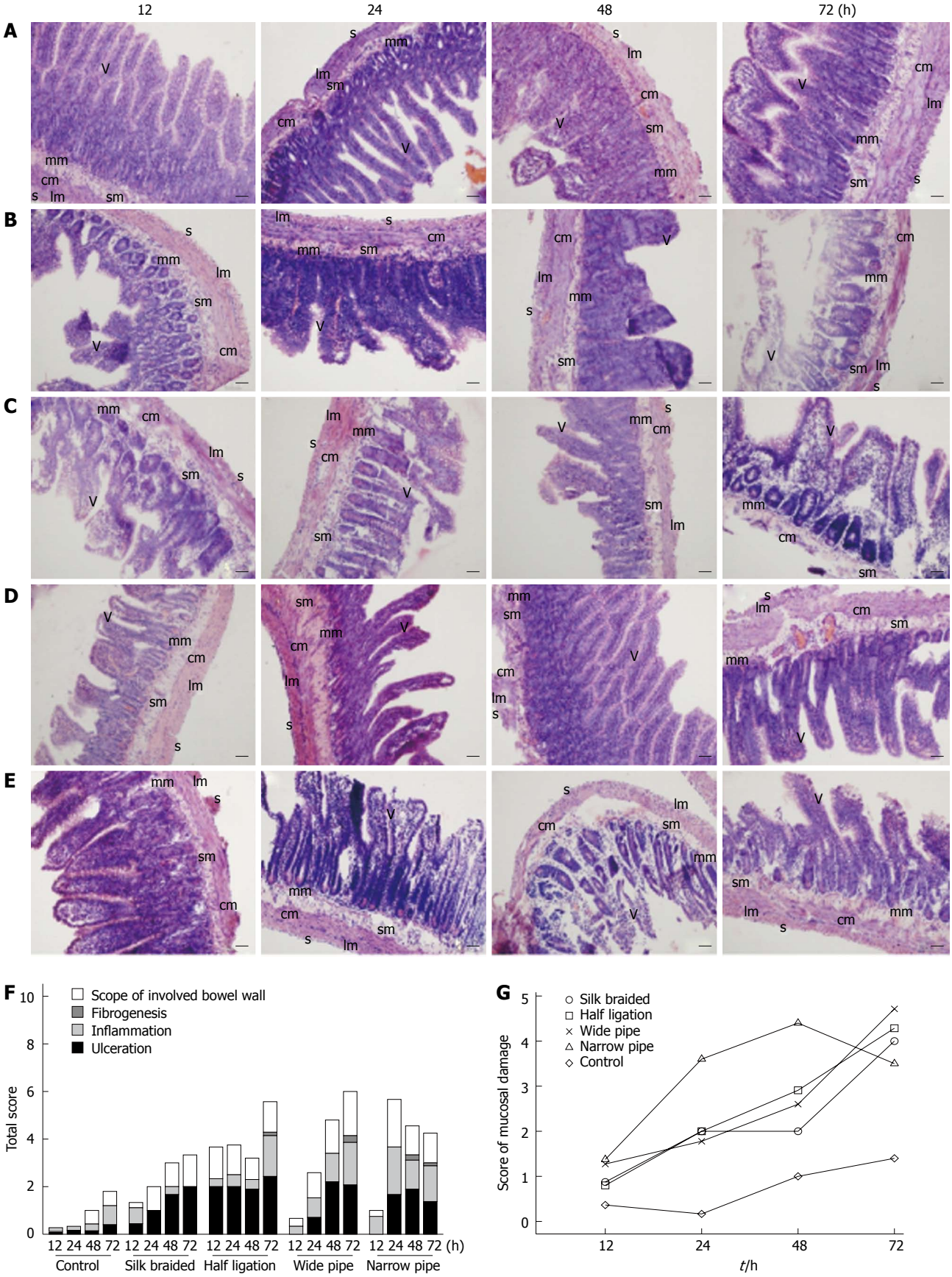

Figure 2 Cross-section of the ileum in obstructed and control rat tissues stained with hematoxylin-eosin. A: Control; B: Braided silk; C: Half ligation; D: Wide pipe; E: Narrow pipe. Rats were killed at different time points after surgery; F: The histopathological score of changes in the extent and severity of ulceration, inflammation, fibrogenesis and scope of involved bowel wall; G: Analytical data of the total scores of intestinal damage following histological mucosal damage in obstructed and control rats. (scale bar: 20 μm).

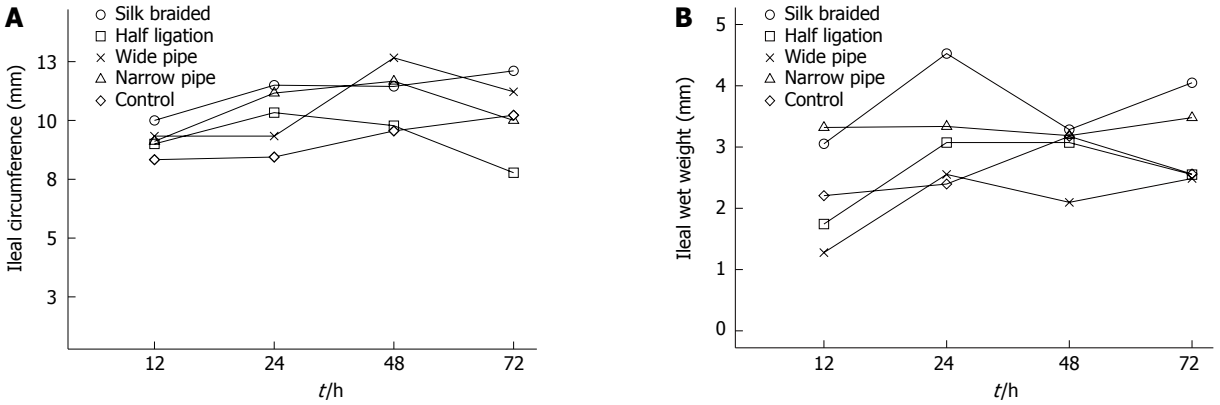

Figure 3 Average ileal wet weight and circumference in the obstructed and control rats. A: The average values for the ileal circumference in the dilated portion of the obstruction rat tissue were significantly larger than those in the corresponding portion of the controls ($P < 0.01$); B: In the obstructed intestine, there was a marked increase in the wet weight due to thickening of the muscle layers. When the groups were compared, these increases were most obvious in the braided silk group, followed by the wide pipe, the narrow pipe group and the half ligation group.

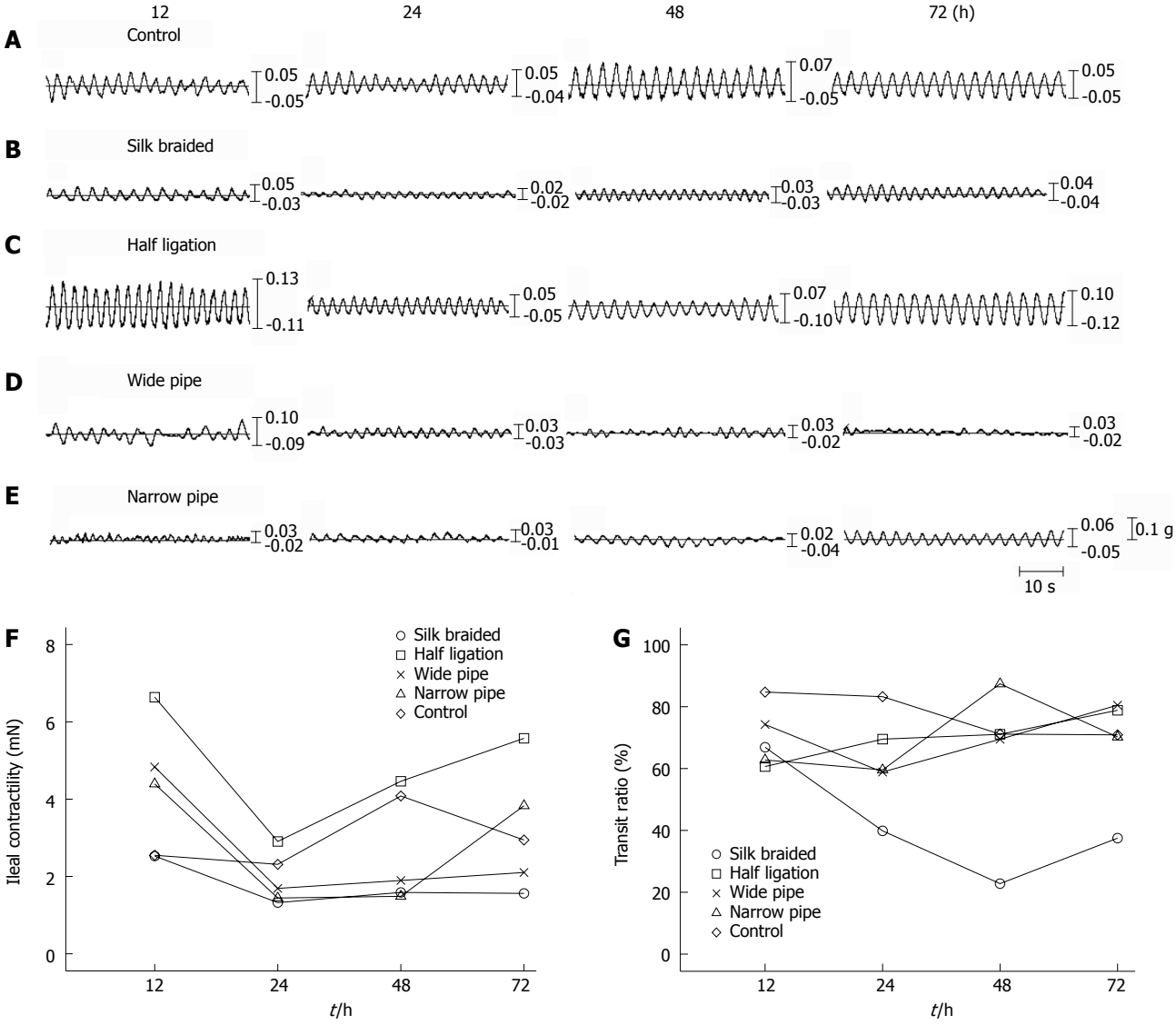

Figure 4 Changes in spontaneous rhythmic contractions. Original traces of rhythmic contractions in obstructed and control ileum. A: Control; B: Braided silk; C: Half ligation; D: Wide pipe; E: Narrow pipe. The data illustrate typical traces of spontaneous contractions at different time points; F: Data showing ileal contractility of spontaneous rhythmic motility; G: Data of intestinal transit ratio showing movement capability *in vivo*.

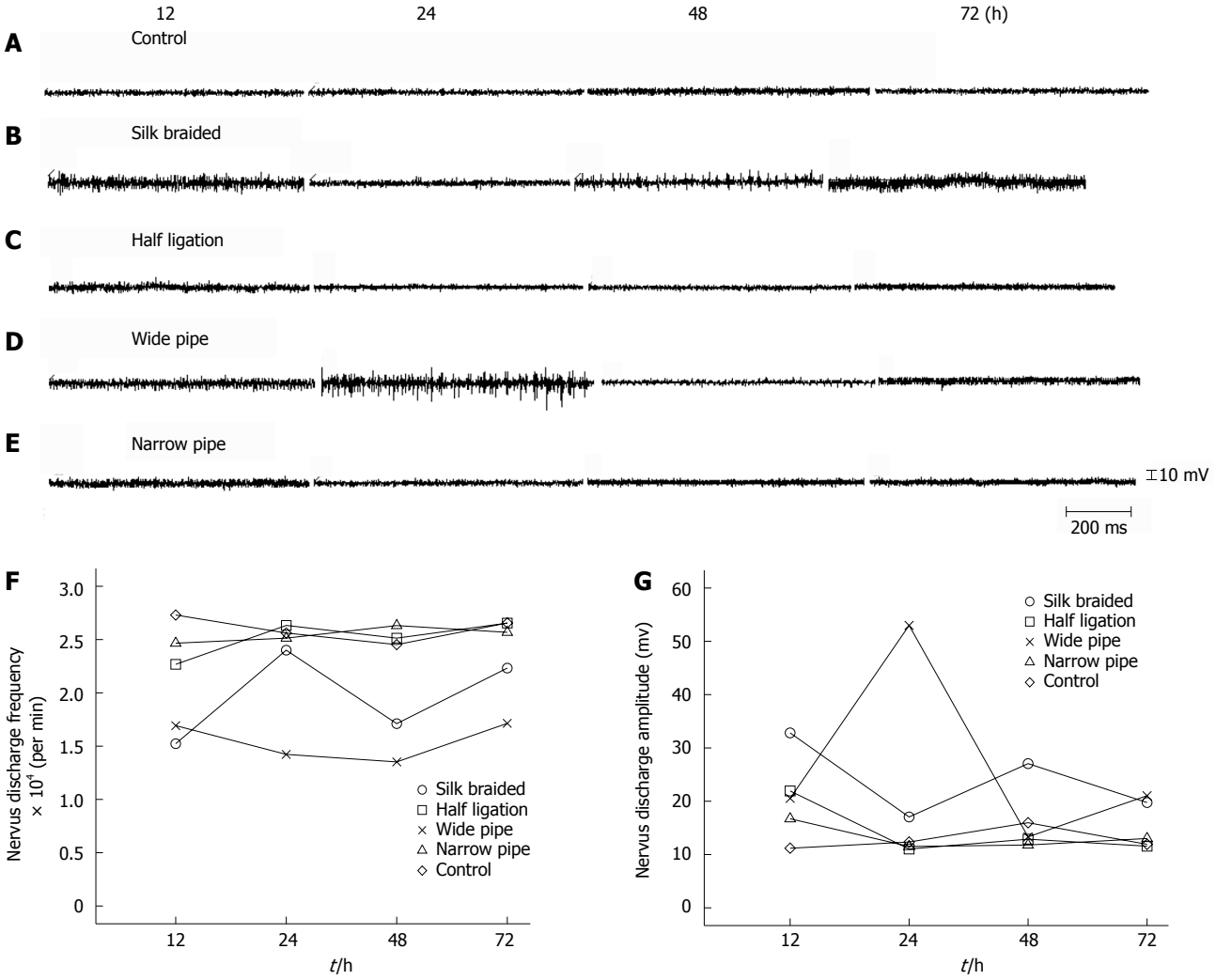

Figure 5 Changes in autonomic nerve electrical discharge. Original traces of the vagus nerve in the obstructed and control ileum. A: Control; B: Braided silk; C: Half ligation; D: Wide pipe; E: Narrow pipe. The data illustrate typical traces of autonomic electrical discharge at different time points; F: Data of frequency of vagus electrical discharge showing autonomic nerve electrical activity; G: Data of amplitude of vagus electrical discharge showing autonomic nerve electrical activity.

half ligation group, the braided silk group and then the wide pipe group which showed a slight decrease at 12 h, but gradually increased from 24 to 72 h. With regard to food intake and feces, these increased in the narrow pipe and half ligation groups compared with the controls. In contrast, the braided silk and wide pipe groups showed significant changes with varying degrees of weight loss or gain ($P < 0.01$). The mental status of the controls, narrow pipe and half ligation groups was good or moderate, however, the braided silk and wide pipe groups displayed the opposite status. Although not statistically significant, the number of deaths was lowest in the control rats. Deaths due to obstruction were higher in the controls, followed by the narrow pipe group the braided silk group, the half ligation group and the wide pipe group. These findings show that the braided silk and wide pipe established the incomplete intestinal obstruction model more successfully, with fewer deaths, than the other models.

Consistent with the findings in other reports[3-6,13-15], the changes in the extent and severity of adhesions, stenosis, ulceration and bowel wall thickness in the obstructed and control rats were assessed using the total scores of intestinal damage following macroscopic evaluation (Figure 1F). The controls (Figure 1A) showed slight intestinal wall thickness and no evidence of intestinal damage. In contrast, obstructed rats showed flushing, tumefaction of intestinal mucosa, hyperemia and hemorrhage of bowel wall and stasis of bowel contents to varying degrees from the proximal region to the site of the ring compared with control rats (Figure 1B-E). Statistically significant differences in the scores of intestinal damage were observed in obstructed rats compared with the controls ($P < 0.01$). Intestinal damage due to the braided silk and narrow pipe was serious as time passed, especially stenosis and ulceration. The half ligation and wide pipe groups showed medium damage at 12 to 72 h.

Some studies reported that intestinal wet weight and circumference were able to reflect the degree of dilation and increased weight of the intestine[15-16], therefore, we

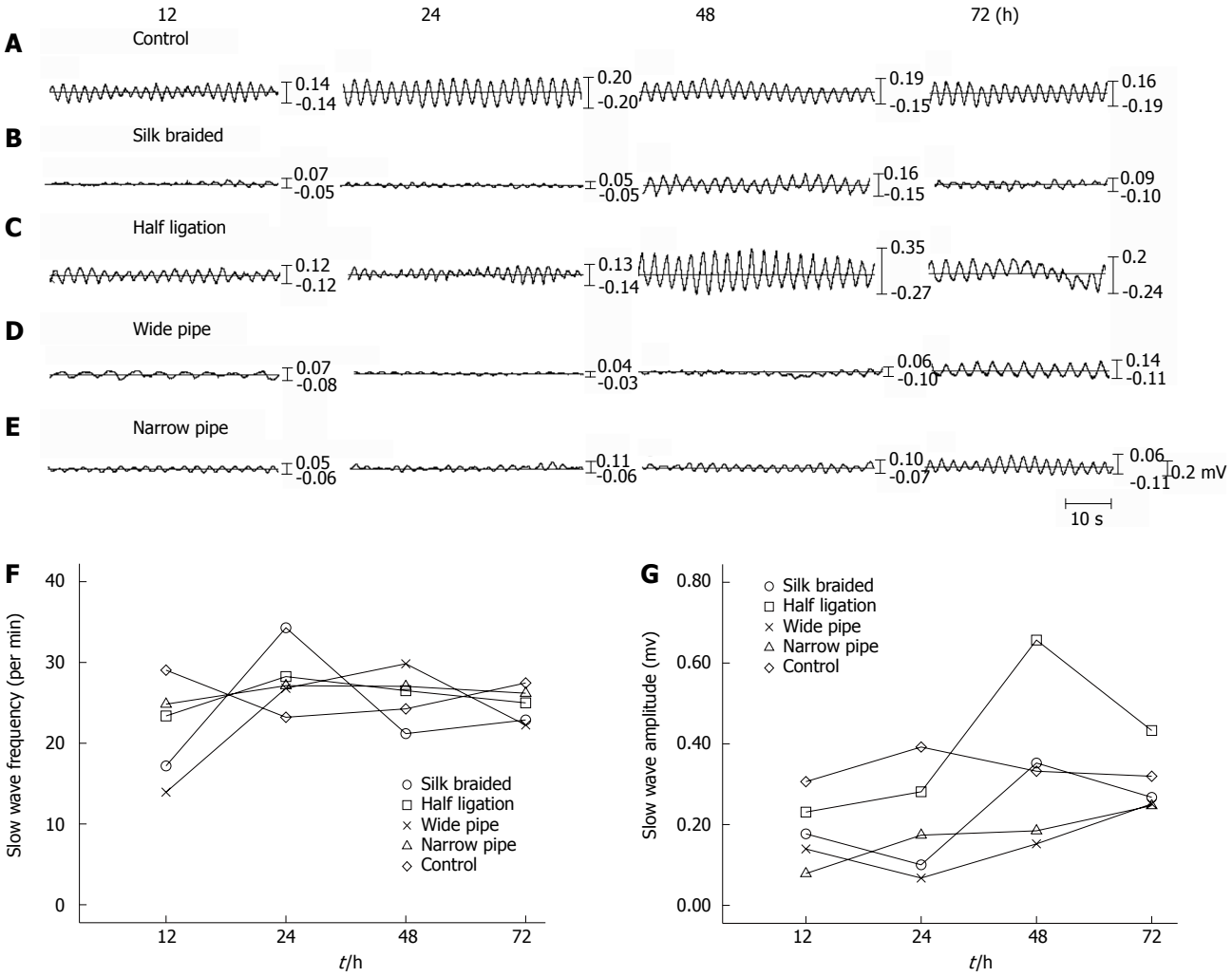

Figure 6 Change in pacemaker activity in the ileum. Typical intracellular electrical activity (slow waves) recorded in the small intestine of control rats and at 12-72 h at the site of intestinal obstruction. A: Control; B: Braided silk; C: Half ligation; D: Wide pipe; E: Narrow pipe; F: Data on slow wave frequency in normal functioning tissue away from the obstruction site; G: Slow-wave amplitude was markedly reduced near the site of obstruction and increased in amplitude in normal functioning tissue away from the obstruction site.

measured the wet weight and circumference of ileum 3 cm distal to the obstruction. In the *in vivo* study, ileal wet weights of the braided silk tissue in the dilated portion were significantly greater ($P < 0.01$) when compared with the controls (Figure 3B). The magnitude of this increase was reduced in the narrow pipe group. In contrast, other obstructed rats showed a decrease compared with those in the corresponding portion of the controls. The ileal circumference showed a negligible increase in both the obstructed and control groups (Figure 3A).

In accordance with the above findings, we speculated that the braided silk and wide pipe models would be useful in the clinic. Therefore, we evaluated the photomicrographs of tissues stained with hematoxylin and eosin (Figure 2), and found that all rats with intestinal obstruction showed ulceration of the mucosa and submucosa, and vascular congestion with focal hemorrhage in the entire tissue layer. In addition, mucosal edema and inflammation were found in the wide pipe and narrow pipe groups, and occasional fibrogenesis in the half ligation, wide pipe and narrow pipe groups at later time periods. Compared with the control rats (Figure 2A), the dilated intestinal region of obstructed rats (Figure 2B-E) showed infiltration of polymorphonuclear cells, plasma cells and neutrophils. A comparison of these scores in the obstructed rats showed that they were significantly different from each other ($P < 0.01$), and the scores were increased in obstructed rats compared with control rats (Figure 2F). Therefore, the braided silk and wide pipe models may better simulate intestinal obstruction found in the clinic.

In the *in vitro* experiments, the braided silk and wide pipe groups demonstrated reduced ileal contractility compared with the controls, the narrow pipe group demonstrated a moderate reduction, and the half ligation group demonstrated an increase in ileal contractility (Figure 4A-B). We observed that the basic spontaneous mechanical contraction activities of dilated intestine *in vivo* and *in vitro* were significantly reduced ($P < 0.01$). The transit ratio in obstructed rats was less than that in con-

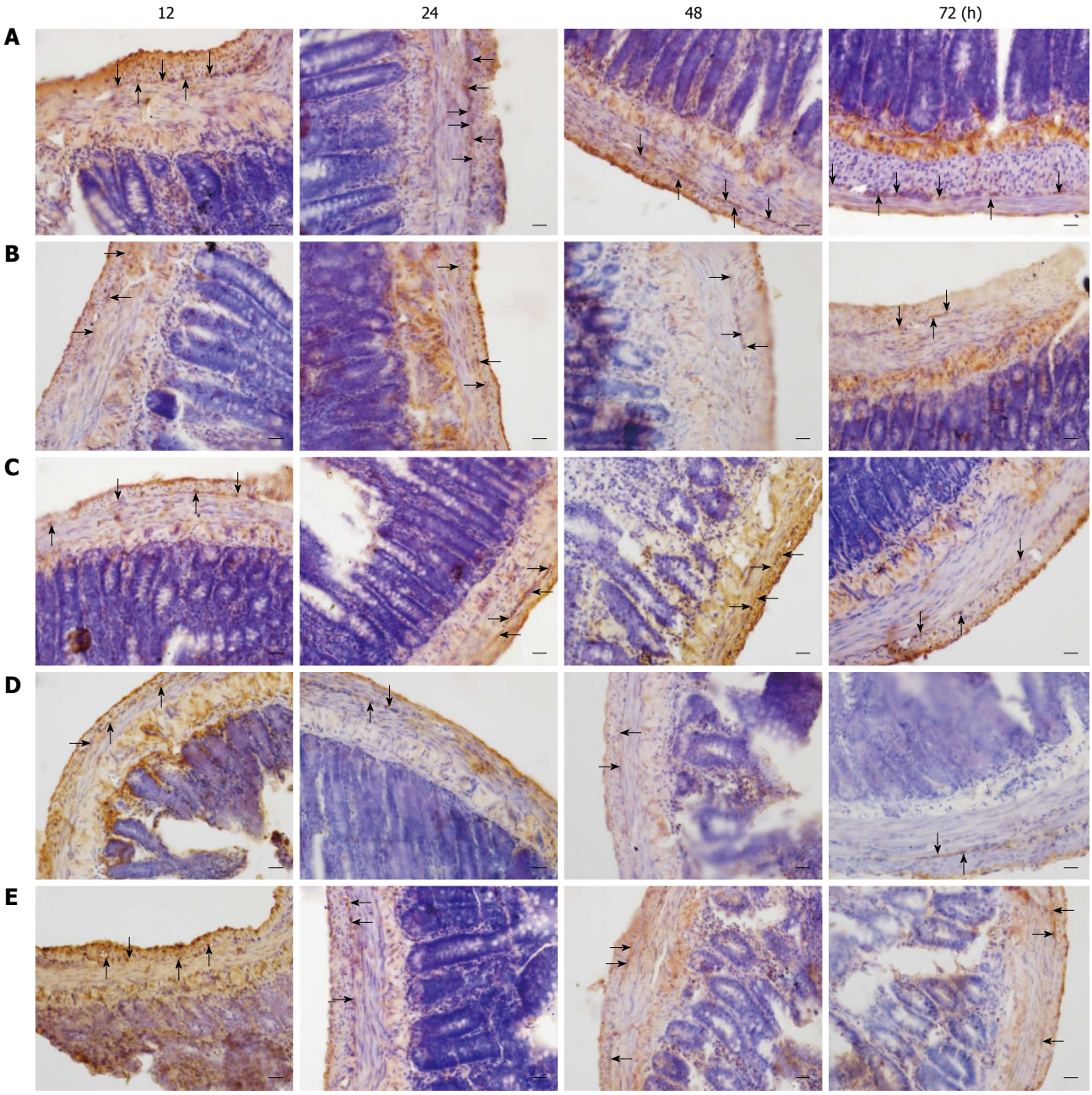

Figure 7 Immunohistochemistry of c-Kit positive interstitial cells of Cajal (arrow) in whole mount preparations of ileum in the obstructed and control rats. A: Control; B: Braided silk; C: Half ligation; D: Wide pipe; E: Narrow pipe. Rats were killed at different time points after surgery. Each panel shows c-Kit positive interstitial cells of Cajal at different times (scale bar: 20 μm).

trols, especially in the braided silk group, and the other obstructed groups showed a smaller reduction in the transit ratio. In contrast to the *in vitro* approach, these *in vivo* studies showed that the incomplete intestinal obstruction models using braided silk and wide pipe were better than the other models, particularly with regard to influence on intestinal movement capability (Figure 4C). These findings are similar to those of Huizinga *et al*[17] who demonstrated that there was a close relationship between intestinal transit and myogenic mechanisms, and indicated that electrical and mechanical activities can influence each other.

Cheng *et al*[18] reported that intestinal motility is an autonomic rhythmic activity under normal circumstances, which is regulated by nerves, hormones and other factors. The autonomic nervous system plays an important role in the regulation of intestinal motility rhythm. External innervation of the intestinal tract is mainly by the vagus nerve, and the sympathetic nerves play a role in balance and coordination[19,20]. In the present study, we compared nerve electrophysiological activity in different models of intestinal obstruction in rats (Figure 5A), to determine the vagus nerve autonomic electrical discharge which represents changes in the complex enteric nervous system. The frequency and amplitude of vagus nerve autonomic electrical discharge in control rats were

Table 3 Summary of daily general condition

General condition	Control				Braided silk				Half ligation				Wide pipe				Narrow pipe			
	12 h	24 h	48 h	72 h	12 h	24 h	48 h	72 h	12 h	24 h	48 h	72 h	12 h	24 h	48 h	72 h	12 h	24 h	48 h	72 h
Body weight (E = 10)	--	→	-		-	→	+		-				-	→	+ +		--			
Food intake (B = 5.0, E = 2.5)	±	→	+		±	→	--		+	→	±		+ +	→	±		-			
Feces																				
Dry weight (B = 1.0, E = 0.50)	-	→	+ +		--				-	→	+ +		-	→	--		-	→	+	
Color	Yellow and black → Yellow				Yellow and black → Black				Yellow and black				Yellow and black				Yellow and black → Yellow			
Pill (B =15, E =10)	±	→	+		--	→	-		±	→	+ +		-	→	--		-	→	+	
Score (B = 20, E = 10)	-	→	+		--	→	-		--	→	+ +		--				+	→	+ +	
Death	+	±	±	±	+	±	++	+	++	±	±	+	+	±	±	+	±	±	++	++

B: Base value; E: Extent of increase and reduction; + +: Wider band increase (> E); +: Narrower band increase (< E); ±: No increase or reduction; -: Narrower band reduction (< E); --: Wider band reduction (> E). The values of the score are equal to pill multiplied by color. The color is defined by Yellow = 1, Yellow and black = 1.5, Black = 2.

normal and rhythmic. Those in the wide pipe group were irregular, moderate in the braided silk group, and were normal at each time point in the half ligation and narrow pipe groups (Figure 5B-C). These results demonstrated that the wide pipe can be used successfully to establish a model of incomplete intestinal obstruction in rats.

Considering the possible link between spontaneous mechanical contraction activities and the slow wave of dilated intestine *in vivo* and *in vitro*[17,21], we investigated the waveform and reflected frequency and amplitude of the slow wave in different rats (Figure 6A). We found that the waveform in the wide pipe group resembled a sine curve and showed a notching wave which was irregular at 12 to 72 h. The half ligation group showed no obvious change in the waveform compared with the controls. Peak amplitudes in the braided silk and narrow pipe groups demonstrated different degrees of weakening. In this study, we also found a close relationship between frequency (Figure 6B) and peak amplitudes (Figure 6C) in the vagus nerve electrical discharge at baseline and intestinal motility. This suggested that the wide pipe model may be similar to human incomplete intestinal obstruction.

It is well known that slow waves are relatively regular periodic electrical activities and the basis of intestinal smooth muscle action potentials. In earlier research, we found that the frequency and amplitude of slow wave propagation were reduced in ileac muscles[6]. Other studies[3,22] showed that myoelectrical rhythm is irregular and the slow waves decrease. In this study, the waveform and reflected frequency and amplitude of the slow wave in control rats were normal. Those in the wide pipe group were irregular, were moderate in the braided silk group, and were normal in the half ligation and narrow pipe groups at 12 to 72 h (Figure 6). These results suggest that slow wave abnormalities are responsible for intestinal motility dysfunction.

In our previous intestinal studies, we observed that the enteric nervous system (ENS) - ICC - smooth muscle cell (SMC) network constitute the basic functional unit of gastrointestinal motility and has an important relationship with spontaneous rhythmic activity[12,14,17-18,23]. We supposed that the wide pipe group abolished the propulsive peristaltic waves in the dilated intestine compared with the other obstructed groups, which caused a significant disturbance in spontaneous rhythmic contractions of intestinal smooth muscle. In smooth muscle, there are several factors which increase the frequency of contraction, such as increased pacemaker activity and shortened action potential[24].

It has been previously shown that ICC are regarded as the pacemaker cells of the gastrointestinal (GI) tract[25-28], which suggests that ICC may play a role in GI motility. In order to compare the differences in obstructed rats, and to identify the mutual influence between the ENS-ICC-SMC networks, we investigated the distribution of ICC in intestinal tissue using light microscopy.

Another interesting observation from this study was that, in the wide pipe group the increase in intestinal contractility was closely related to a reduction in the number of ICC and slow wave, which was different in the other obstructed groups. In addition, it was reported that a reduction in the frequency of rhythmic contractions was connected to the disruption of ICC in the dilated intestine of obstructed rats[29]. These findings confirmed those in our study (Figure 7). Therefore, it is likely that ICC lost their original cell phenotype, resulting in an increase in the number of smooth muscle cell-like cells, thereby improving contractility of the ileum. At the present time, we do not know the precise mechanisms underlying such alterations. Further study will be needed to clarify this point.

In conclusion, the results of the present study suggest that there are significant differences *in vivo* and *in vitro* among the four animal models of incomplete intestinal obstruction. The pathogenic mechanism and clinical features in the different models have essential distinctions. Despite being of a similar general condition, the rats in each group showed differences including macroscopic and histological presentation, intestinal transit ratio and contractility, circumference and wet

weight, amplitude and frequency of nerve electrical discharge and slow wave, and ICC numbers. These findings may allow use of the wide pipe to establish a model that is approximate to human incomplete intestinal obstruction. However, a detailed analysis of this is necessary based on the characteristics of the different models used in this study which can be used as a reference.

ACKNOWLEDGMENTS

We greatly thank Zhang Xiao of our department for their technical assistance with the present study.

COMMENTS

Background

Considering the impairment associated with incomplete intestinal obstruction, the use of animal models is now a focus in this research field, however, to date, no particular model parallels the complex nature of human intestinal obstruction.

Research frontiers

Animal have been used to establish incomplete intestinal obstruction models. However, animal models are not been widely used and research comparing the characteristics in different rat models is rare. In this study, the authors successfully established a reliable animal model and demonstrated that the wide pipe rat model is similar to human incomplete intestinal obstruction.

Innovations and breakthroughs

Recent reports have highlighted the need to establish a reliable animal model of intestinal obstruction. Different types of materials are currently available. This is the first experimental study to compare rat models of incomplete intestinal obstruction. Furthermore, the authors obtained electrophysiologic, morphologic and histologic information which may have some clinical relevance.

Applications

These findings may provide a valuable theoretical basis for selecting incomplete intestinal obstruction models with better feasibility and reproducibility.

Peer review

This is an animal model study which comprehensively demonstrates the results. Overall, it is suitable for publication.

REFERENCES

1 **Kulaylat MN**, Doerr RJ. Small bowel obstruction. In: Holzheimer RG, Mannick JA. Surgical Treatment: Evidence-Based and Problem-Oriented. Munich: Zuckschwerdt, 2001, cited 2012-05-21. Available from: URL: http//www.ncbi.nlm.nih.gov/ books/NBK6873/.

2 **Kibayashi K**, Sumida T, Shojo H, Tokunaga O. Unexpected death due to intestinal obstruction by a duplication cyst in an infant. *Forensic Sci Int* 2007; **173**: 175-177 [PMID: 17236734 DOI: 10.1016/j.forsciint.2006.12.010]

3 **Chang IY**, Glasgow NJ, Takayama I, Horiguchi K, Sanders KM, Ward SM. Loss of interstitial cells of Cajal and development of electrical dysfunction in murine small bowel obstruction. *J Physiol* 2001; **536**: 555-568 [PMID: 11600689 DOI: 10.1111/j.1469-7793.2001.0555c.xd]

4 **Yang S**, Shen L, Jin Y, Liu J, Gao J, Li D. Effect of Dachengqi decoction on NF-kappaB p65 expression in lung of rats with partial intestinal obstruction and the underlying mechanism. *J Huazhong Univ Sci Technolog Med Sci* 2010; **30**: 217-221 [PMID: 20407877]

5 **Collins J**, Vicente Y, Georgeson K, Kelly D. Partial intestinal obstruction induces substantial mucosal proliferation in the pig. *J Pediatr Surg* 1996; **31**: 415-419 [PMID: 8708915 DOI: 10.1016/S0022-3468(96)90750-2]

6 **Yuan ML**, Yang Z, Qiu YB, Guo JL, Huang YQ, Kang X, Cheng JJ, Xi L, Zhou Y, Zhang Y, Chen Y, Gong D, Zhang X. Effects of Raphanus Sativus Extract on Intestine Slow Waves of Incomplete Intestinal Obstruction in Rats. *Lishizhen Med and Materia Med Res* 2012; **23**: 952-954

7 **Institute for Laboratory Animal Research**. Guide for the care and use of laboratory animals. 8th ed. Washington DC: National Academies Press, 2011: 168-173

8 **Butzner JD**, Parmar R, Bell CJ, Dalal V. Butyrate enema therapy stimulates mucosal repair in experimental colitis in the rat. *Gut* 1996; **38**: 568-573 [PMID: 8707089 DOI: 10.1136/gut.38.4.568]

9 **Chiu CJ**, McArdle AH, Brown R, Scott HJ, Gurd FN. Intestinal mucosal lesion in low-flow states. I. A morphological, hemodynamic, and metabolic reappraisal. *Arch Surg* 1970; **101**: 478-483 [PMID: 5457245 DOI: 10.1001/archsurg.1970.01340280030009]

10 **Tomita R**. Regulation of the peptidergic nerves (substance P and vasoactive intestinal peptide) in the colon of women patients with slow transit constipation: an in vitro study. *Hepatogastroenterology* 2008; **55**: 500-507 [PMID: 18613396]

11 **Sanders KM**, Ordög T, Koh SD, Torihashi S, Ward SM. Development and plasticity of interstitial cells of Cajal. *Neurogastroenterol Motil* 1999; **11**: 311-338 [PMID: 10520164 DOI: 10.1046/j.1365-2982.1999.00164.x]

12 **Takaki M**. Gut pacemaker cells: the interstitial cells of Cajal (ICC). *J Smooth Muscle Res* 2003; **39**: 137-161 [PMID: 14695026 DOI: 10.1540/jsmr.39.137]

13 **Won KJ**, Suzuki T, Hori M, Ozaki H. Motility disorder in experimentally obstructed intestine: relationship between muscularis inflammation and disruption of the ICC network. *Neurogastroenterol Motil* 2006; **18**: 53-61 [PMID: 16371083]

14 **Ward SM**, Sanders KM. Physiology and pathophysiology of the interstitial cell of Cajal: from bench to bedside. I. Functional development and plasticity of interstitial cells of Cajal networks. *Am J Physiol Gastrointest Liver Physiol* 2001; **281**: G602-G611 [PMID: 11518672]

15 **Shroyer NF**, Helmrath MA, Wang VY, Antalffy B, Henning SJ, Zoghbi HY. Intestine-specific ablation of mouse atonal homolog 1 (Math1) reveals a role in cellular homeostasis. *Gastroenterology* 2007; **132**: 2478-2488 [PMID: 17570220 DOI: 10.1053/j.gastro.2007.03.047]

16 **Dou Y**, Fan Y, Zhao J, Gregersen H. Longitudinal residual strain and stress-strain relationship in rat small intestine. *Biomed Eng Online* 2006; **5**: 37 [PMID: 16759387]

17 **Huizinga JD**, Ambrous K, Der-Silaphet T. Co-operation between neural and myogenic mechanisms in the control of distension-induced peristalsis in the mouse small intestine. *J Physiol* 1998; **506** (Pt 3): 843-856 [PMID: 9503342 DOI: 10.1111/j.1469-7793.1998.843bv.x]

18 **Cheng W**, Lui VC, Chen QM, Tam PK. Enteric nervous system, interstitial cells of cajal, and smooth muscle vacuolization in segmental dilatation of jejunum. *J Pediatr Surg* 2001; **36**: 930-935 [PMID: 11381429 DOI: 10.1053/jpsu.2001.23979]

19 **Gao Z**, Müller MH, Karpitschka M, Mittler S, Kasparek MS, Renz B, Sibaev A, Glatzle J, Li Y, Kreis ME. Role of the vagus nerve on the development of postoperative ileus. *Langenbecks Arch Surg* 2010; **395**: 407-411 [PMID: 20333399 DOI: 10.1007/s00423-010-0594-5]

20 **Balemba OB**, Hay-Schmidt A, Assey RJ, Kahwa CK, Semuguruka WD, Dantzer V. An immunohistochemical study of the organization of ganglia and nerve fibres in the mucosa of the porcine intestine. *Anat Histol Embryol* 2002; **31**: 237-246 [PMID: 12196267 DOI: 10.1046/j.1439-0264.2002.00403.x]

21 **Huizinga JD**. Physiology and pathophysiology of the interstitial cell of Cajal: from bench to bedside. II. Gastric motility: lessons from mutant mice on slow waves and in-

nervation. *Am J Physiol Gastrointest Liver Physiol* 2001; **281**: G1129-G1134 [PMID: 11668020]
22 **Shafik A**, El-Sibai O, Shafik AA, Ahmed I. Electric activity of the colon in irritable bowel syndrome: the 'tachyarrhythmic' electric pattern. *J Gastroenterol Hepatol* 2004; **19**: 205-210 [PMID: 14731132 DOI: 10.1111/j.1440-1746.2004.03279.x]
23 **Camilleri M**, Lee JS, Viramontes B, Bharucha AE, Tangalos EG. Insights into the pathophysiology and mechanisms of constipation, irritable bowel syndrome, and diverticulosis in older people. *J Am Geriatr Soc* 2000; **48**: 1142-1150 [PMID: 10983917]
24 **Wray S**. Uterine contraction and physiological mechanisms of modulation. *Am J Physiol* 1993; **264**: C1-18 [PMID: 8430759]
25 **Huizinga JD**, Thuneberg L, Klüppel M, Malysz J, Mikkelsen HB, Bernstein A. W/kit gene required for interstitial cells of Cajal and for intestinal pacemaker activity. *Nature* 1995; **373**: 347-349 [PMID: 7530333]
26 **Sanders KM**. A case for interstitial cells of Cajal as pacemakers and mediators of neurotransmission in the gastrointestinal tract. *Gastroenterology* 1996; **111**: 492-515 [PMID: 8690216 DOI: 10.1053/gast.1996.v111.pm8690216]
27 **Sanders KM**, Ordög T, Ward SM. Physiology and pathophysiology of the interstitial cells of Cajal: from bench to bedside. IV. Genetic and animal models of GI motility disorders caused by loss of interstitial cells of Cajal. *Am J Physiol Gastrointest Liver Physiol* 2002; **282**: G747-G756 [PMID: 11960771]
28 **Ward SM**, Sanders KM, Hirst GD. Role of interstitial cells of Cajal in neural control of gastrointestinal smooth muscles. *Neurogastroenterol Motil* 2004; **16** Suppl 1: 112-117 [PMID: 15066015 DOI: 10.1111/j.1743-3150.2004.00485.x]
29 **Lou Z**, Li JS. Interstitial cells of Cajal in abdominal sepsis and hypertension-induced ileus in rats. *Eur Surg Res* 2009; **43**: 47-52 [PMID: 19439971 DOI: 10.1159/000218102]

P- Reviewers Losanoff JE, Kate V **S- Editor** Wen LL
L- Editor A **E- Editor** Zhang DN